A Hybrid Stochastic Model for Characterization of Subsurface Heterogeneity.

Amr ElFeki

Irrigation and Hydraulics Engineering Department., Faculty of Engineering., El-Mansoura University., El-Mansoura., Egypt.

A HYBRID STOCHASTIC MODEL FOR CHARACTERIZATION OF SUBSURFACE HETEROGENEITY

لموذج أحتمالي تهجيني لتوصيف عدم التجانس الجيولوجي للطبقات تحت السطحية

A.M. M. Elfeki

Lecturer at Irrigation and Hydraulics. Dept., Faculty of Engineering,
El-Mansoura University, El-Mansoura, Egypt.

: الخلاصة

تفرح عده الدرسة طريقه لتوصيف عدم التجانس الجيولوجي للطبقات تحت السطحية باستخدام مدخل تهجيني. يتضمن المدخل التهجيسى الجمع بين البيانات الجيولوجيه عن الطبقات والقياسات الهيدروليكيه لخصائص هذه الطبقات (مثل معامل النفادية) لتوصيف عدم التجانس الجيولوجى للطبقات تحت السطحية . باستخدام هذه الطريقه يتم توصيف الاشكال الهندسيه للتكوينات الجيولوجيه باستخدام نموذج ماركوف المزدوج والذي تم تطويره من قبل المؤلف وآخرين ، وبما تستخدم القياسات الهيدروليكيه للطبقات لتوصيف التغييره داخل كل طبقه من الطبقات الجيولوجية باستخدام نظرية الحقول العشوائية .

أوضحت التجارب العددية التي أجريت بهذا النموذج والذي يدعى (MARKOVTB) ميزات هذا النموذج في توليد تكوينات جيولوجيه ذات خصائص متعدده وإبعا القدره على تمسير البيانات الحقليه للمواقع المختلمه.

ABSTRACT

This study proposes a methodology for characterization of subsurface heterogeneity using a hybrid approach. The hybrid approach will incorporate soft geological information in addition to the available hard data to characterise geological heterogeneity under two scales of variability. The geometric shapes of the geological features are modelled stochastically based on soft information using the Coupled Markov Model developed by Elfeki et al. (1995), while hard data are used to model the variability inside these geometric shapes. This will lead to an improved characterization of the subsurface heterogeneity. The proposed hybrid model can be used to generate realizations of conductivity within the geological structure, with all realizations satisfying the "soft" geological knowledge and "hard" data.

INTRODUCTION

Long time scale predictions by flow and transport models rely strongly on the appropriate description of the spatial structures of subsurface formations at various scales. These predictions are of utmost importance in connection with groundwater resource management. Detailed knowledge of the subsurface variability is never available in a deterministic sense. An alternative is stochastic modelling. A problem in stochastic methods is that the actual formation is often modelled by unimodal stationary random fields and, as a consequence, much of the actual spatial structure is lost. Moreover, stationary fields are unrealistic in many geological settings. In practice, the natural variability observed in geological formations is nested, i.e., a geometric structure is most often manifested with other internal fluctuations superimposed over the structure (e.g. Journel, et al., 1978). This practical situation is not addressed in the geohydrological literature. From practical and economical point of view, it may not be feasible to fully characterise formation heterogeneity using hard data. Some authors (Gelhar, 1986; Journel, 1978) have suggested to incorporate subjective or soft data. This study is an attempt to integrate subjective geological information with measurements of hydraulic parameters (hard data).

STAGES OF THE HYBRID MODEL

Geometric Modelling of Large Scale Variability

The purpose of this model is to identify geological features with discrete nature. The coupled Markov model is used to characterise this scale of variability. The geological information is coded in terms of transition probabilities to feed the computer programme "GEOSIM1" developed by the author. For illustration of the model reference is made to Elfeki (1996).

Geostatistical Modelling of Local Scale Variability

The turning bands method applied by Tompson, et al., (1989) is used in this study to generate stationary fields of hydraulic conductivity within each geological unit. The log-conductivity field inside each unit is assumed to be independent from any other unit and it is modelled as

$$Y(x) = \langle Y(x) \rangle + Y'(x) \tag{1}$$

where, $x=(x,y)$ is a position inside a lithological unit, $Y(x)$ is log-conductivity at position x, $\langle Y(x) \rangle$ is the expected value of log-conductivity at position x and $Y'(x)$ is the stationary Gaussian field with an expected value equal to zero and a variance equal to $\sigma^2_{Y(x)}$. The field of $Y(x) = log(K(x))$ in the various units is transformed into a field of $K(x)$ by :

$$K(x) = \exp[Y(x)] \tag{2}$$

The spatial structure of the log-conductivity field in each geological unit is specified by an anisotropic exponential autocovariance function.

IMPLEMENTATION OF THE HYBRID MODEL

Generation of The Geological Structure(Megascale Heterogeneity)

The geological structure is sampled over intervals of a coarse grid. Transition probabilities between the different lithologies are determined and used for the simulation. A brief description of the steps are given here. The left and top boundaries are generated by the horizontal and vertical chains respectively in the same way as described by Elfeki (1996) At each cell location in the domain, the conditional probabilities of the coupled chains are calculated for all the states. A cumulative distribution of transition probabilities from the coupled chains is built. Monte-Carlo sampling to realise the states of the cell given the states of the neighbours is applied. The procedure is repeated until all cells of the simulation grid are assigned a state.

Generation of Local Variability (Macroscopic Heterogeneity)

A finer grid is superimposed over the geological structure and each cell in the grid is coded with the prescribed lithology. A search algorithm is followed for assignment of values of hydraulic conductivity to each geological unit in the system. The following steps are considered. If x is positioned in lithology S_k, then $Y(x) = \langle Y_k \rangle + Y'_k$, $k = 1,..., n$, where Y'_k is a statistically homogeneous Gaussian random field, generated by the turning bands algorithm.

The search algorithm is repeated to cover all the cells in the domain and each cell is assigned a value corresponds to parameters of its statistical distribution and its statistical anisotropy pattern. Then the conductivity value is calculated by the anti-logarithm as, $K(\mathbf{x}) = exp(Y(\mathbf{x}))$.

ILLUSTRATION OF THE MODEL RESULTS BY SOME SYNTHETIC EXAMPLES

A set of non-stationary two-dimensional fields is generated by the models "GEOSIM1" and "MARKOVTB".developed by the author. The model is illustrated in Fig. 1. Here, a 2D vertical cross-section of large scale geological structure is shown with dimensions of 2000 m in length and 400 m in depth (see top of Fig 1). It is assumed that the geological system consists of four lithological units coded 1, 2, 3 and 4 in the figure and indicated by colour white, light grey, dark grey and black respectively. The structure is generated by the Markov method with transition probabilities given in Table 1, sampled over intervals of 20 m in the horizontal direction and 10 m in the vertical direction. A finer grid with cell dimensions of 10 x 5 m is superimposed over the structure for the generation of conductivity field. The conductivity variations inside each geological unit is generated by the computer model " MARKOVTB" with various statistics in order to investigate various cases of non-stationary fields. Parameters of each case are displayed in tables 2, 3, 4, 5 respectively The simulation results of these cases will be discussed in the following sections.

Table 1 Statistics used to generate the geological structure in Fig 1.

Length of the given section (m)= 2000 ,   Depth of the given section (m) = 400
Sampling interval in X-axis (m) =   20   Sampling interval in Y-axis (m)=10.

Horizontal Transition Probability Matrix

State	Input Statistics to the Model				Calculated Statistics from Fig.1a			
	1	2	3	4	1	2	3	4
1	0.960	0.010	0.010	0.020	0.933	0.007	0.021	0.039
2	0.010	0.970	0.010	0.010	0.015	0.964	0.012	0.009
3	0.010	0.020	0.960	0.010	0.006	0.026	0.957	0.011
4	0.010	0.010	0.010	0.970	0.016	0.002	0.014	0.968

Vertical Transition Probability Matrix

State	Input Statistics to the Model				Calculated Statistics from Fig.1a			
	1	2	3	4	1	2	3	4
1	0.930	0.010	0.030	0.030	0.810	0.041	0.053	0.096
2	0.100	0.800	0.050	0.050	0.044	0.876	0.071	0.010
3	0.050	0.050	0.800	0.100	0.042	0.068	0.805	0.086
4	0.020	0.050	0.040	0.870	0.019	0.077	0.058	0.846

DISCUSSION OF THE MODEL RESULTS

Case (a): Non-Stationarity in The Mean

It is assumed that each geological unit possesses a different mean conductivity, while the variance and correlation lengths are assumed equal. The simulation parameters used are displayed in Table 2. Fig. 2a shows some conductivity profiles. In Fig. 1a it can be seen that the boundaries between the geological units are still clear and not smeared by the influence of the local variability, in this case due to the large contrast in the mean.

Table 2 Simulation Parameters (Non-Stationarity in The Mean).

Parameter State	w_i	$\langle K \rangle$ m/day	σ_K m/day	$\langle Y \rangle$	σ_Y	λ_x (m)	λ_v (m)
1	0.13	100.	10.	4.6	0.10	200.	50.
2	0.31	50.	10.	3.9	0.20	200.	50.
3	0.31	10.	10.	1.96	0.83	200.	50.
4	0.25	1.	10.	-2.3	2.15	200.	50.

where, w_i is the marginal probability of state i, $\langle K \rangle$ is the mean conductivity of state i, σ_K is the standard deviation of state i, $\langle Y \rangle$ is the logarithmic transform of $\langle K \rangle$, σ_Y is the log-transform of $\sigma_{K.}$, λ_x and λ_y are the correlation lengths of each state in x and y directions respectively.

Case (b): Non-Stationarity in The Variance

It is assumed that the geological units possess different conductivity variances, while the arithmetic mean and the correlation lengths are constant. The simulation parameters used are displayed in Table 3. Fig.2b shows a conductivity profile In Fig. 1b it can be seen that the structure is smeared by the variability.

Table 3 Simulation Parameters (Non-Stationarity in The Variance).

Parameter State	w_i	$\langle K \rangle$ m/day	σ_K m/day	$\langle Y \rangle$	σ_Y	λ_x (m)	λ_v (m)
1	0.13	5.	20.	0.19	1.68	100.	10.
2	0.31	5	10.	0.80	1.27	100.	10.
3	0.31	5.	5.	1.26	0.83	100	10.
4	0.25	5.	2.	1.54	0.39	100.	10.

Case (c): Non-Stationarity in The Correlation Lengths

It is assumed that the geological units possess different correlation lengths but the arithmetic mean of conductivity, the variance and the shape of the auto-covariance function are equal. The parameters used are displayed in Table 4. Fig.1c shows the conductivity field and Fig.2c shows a conductivity profile. In these figures it can be seen that the boundaries are smeared, but from the local variability one can notice different correlation patterns in the generated field.

Table 4 Simulation Parameters (Non-Stationarity in Correlation Lengths).

Parameter State	w_i	$\langle K \rangle$ m/day	σ_K m/day	$\langle Y \rangle$	σ_Y	λ_x (m)	λ_v (m)
1	0.13	10.	5.	2.19	0.47	50.	50.
2	0.31	10.	5.	2.19	0.47	100.	50.
3	0.31	10.	5.	2.19	0.47	200.	10.
4	0.25	10.	5.	2.19	0.47	500.	5.

Case (d): Globally Non-Stationarity

It is assumed that the geological units possess different parameters: arithmetic mean of hydraulic conductivity, variance and correlation lengths, while the auto-covariance functions are equal. This case represents a real field situation. The simulation parameters used are displayed in Table 5. Fig.1d shows the conductivity field generated and Fig.2d shows a conductivity profile. In these figures it can be seen that the boundaries are remarkable like case (a). The non-stationarity in the mean is therefore the major reason of having pronounced boundaries.

Table 5 Simulation Parameters (Globally Non-Stationarity).

Parameter State	w_i	$\langle K \rangle$ m/day	σ_K m/day	$\langle Y \rangle$	σY	λ_x (m)	λ_v (m)
1	0.13	50.	50.	3 57	0.83	50.	50.
2	0.31	10.	5.	2.19	0.47	100.	50.
3	0.31	1.0	2.	-0.80	1.0	200.	20.
4	0.25	0.1	0.5	-3.93	1.81	500.	5

Interpretation of The Model Results by Variogram Analysis

Variograms of log (K) have been estimated in x direction for all previous cases in order to interpret the influence of various types of non-stationarity on the global variogram behaviour. This may help in analysing variograms of real field situation. Fig.4 displays variograms of all cases mentioned earlier, in x direction. For all the cases mentioned above, equivalent globally stationary fields are generated to evaluate the validity of the global-stationarity assumption. The fields are presented in Fig.3. The variograms of the fields are calculated and plotted in Fig.4 for comparisons. Table 6 displays the statistical parameters used to generate the equivalent stationary fields.

Table 6 Simulation Parameters for Equivalent Global Stationary Fields.

Parameter Case	$\langle K_m \rangle$ m/day	σ_m m/day	$\langle Y_m \rangle$	$\sigma_m Y$	$\langle \lambda_x \rangle$ (m)	$\langle \lambda_v \rangle$ (m)
a	31.85	34.5	3.07	0.881	200.	50.
b	5	10.8	0.74	1.32	100.	10.
c	10.	5.	2.19	0.47	224.5	26.
d	9.935	26 3	1.26	1.44	224.5	29.5

where, $\langle K_m \rangle$ is the global mean of the states, σ_m is the global standard deviation of the states, $\langle Y_m \rangle$, $\sigma_m Y$ are the corresponding log-transforms, and $\langle \lambda_x \rangle$, $\langle \lambda_y \rangle$ are the average correlation lengths of the states.

In case (a), non-stationarity in the mean, the non-stationarity in the variogram is most pronounced compared with the other cases, since the variogram does not seem to reach a constant value (sill) and it is growing with the spatial lag. From Fig.4a it is clear that the stationary variogram is far from the non-stationary variogram, which means that the assumption of globally stationarity field in this case is not applicable.

In case (b), non-stationarity in the variance, the non-stationarity behaviour is less pronounced. The reason for that is the influence of high variances and constant mean which smear the

boundaries between the different geological units. This can be observed clearly in the profiles of Fig.2b. Fig.4b shows a reasonable agreement (practically) between variogram shapes in case of non-stationarity and globally stationary field. One can notice that the use of an equivalent globally stationary field to represent the non-stationary is not proper although the variogram shapes look relatively close at further lags. This means that sometimes non-stationarity of the data cannot be observed clearly in the variogram.

In case (c), non-stationarity in the correlation lengths, the variogram looks quite stationary. This means that there is no significant influence of non-stationarity of the correlation patterns of the individual units on the global variogram behaviour. Estimation of the (asymptotic) sill variance from Fig.4c, which is about 0.22 is in perfect agreement with the variance from Table 4 that is $(0.47)^2 = 0.221$. This ensures good reproduction of the variance in the simulated field. Fig 4c shows a relatively fair agreement in the variorgam shapes in case of the non-stationary field and its equivalent globally stationary field. This indicates that non-stationarity in correlation patterns can not be observed in the variogram.

In case (d), globally non-stationarity, the variograms in Fig.4d is far apart, as similar to case (a). This can be attributed to the distinction in the mean conductivities of different geological units which are quite pronounced. The assumption of equivalent stationarity field does not hold, which means that serious errors can be introduced due to neglecting non-stationarity.

CONCLUSIONS

The following concluding remarks are drawn from the study:

(1) Geological knowledge and expertise of subjective nature (translated into transition probabilities) can be combined with quantitative geostatistical models (in terms of correlated random fields) to produce more accurate realizations of lithology and hydraulic conductivity fields of underground reservoirs.

(2) The proposed hybrid model can be used to generate realizations of conductivity within the geological structure, with all realizations satisfying the "soft" geological knowledge (reproduction of transition probabilities) and "hard" data (reproduction of PDFs and its moments).

(3) From the synthetic examples, it has been shown that high contrast in the mean of individual populations is the main factor of pronounced non-stationarity in comparison with other types of non-stationarity.

(4) The assumption of a globally stationary random function model is not adequate to describe many fields as far as the non-stationarity in the mean is concerned.

(5) Unless the non-stationarity of the data is clearly pronounced, it can not be manifested by variogram analysis.

REFERENCES

1. ELFEKI, A. M. & UFFINK, G. J. M. & BARENDS, F. J. B. (1995). Stochastic simulation of heterogeneous geological formations using soft information, with an application to groundwater. In Groundwater Quality: Remediation and Protection, QG'95. Edited by Kovar, K. and Krasny, IAHS Publication No. 225.

2 ELFEKI, A.M. (1996) Stochastic characterization of geological heterogeneity and its impact on groundwater contaminant transport, PhD. thesis at Delft University of Technology, The Netherlands.

3. GELHAR, L. W. (1986). Stochastic subsurface hydrology: from theory to applications. Water Resources. Research. 22(9): 135S-145S.

4 JOURNEL, A. G. & HUIJBREGTS, C. (1978) Mining geostatistics. New York: Academic Press, 600p.

5. TOMPSON, A. F. B. & ABABOU, R. & GELHAR, L. W. (1989) Implementation of the three-dimensional turning bands random field generator Water Resources Research. 25(10): 2227-2243

6. Christakos, G. (1992). Random Fields Models in Earth Sciences Academic, San Diego, Calif

7 Haldorsen, H. H & Damsleth, E (1990). Stochastic Modelling Society of Petroleum Engineers, SPE 20321.
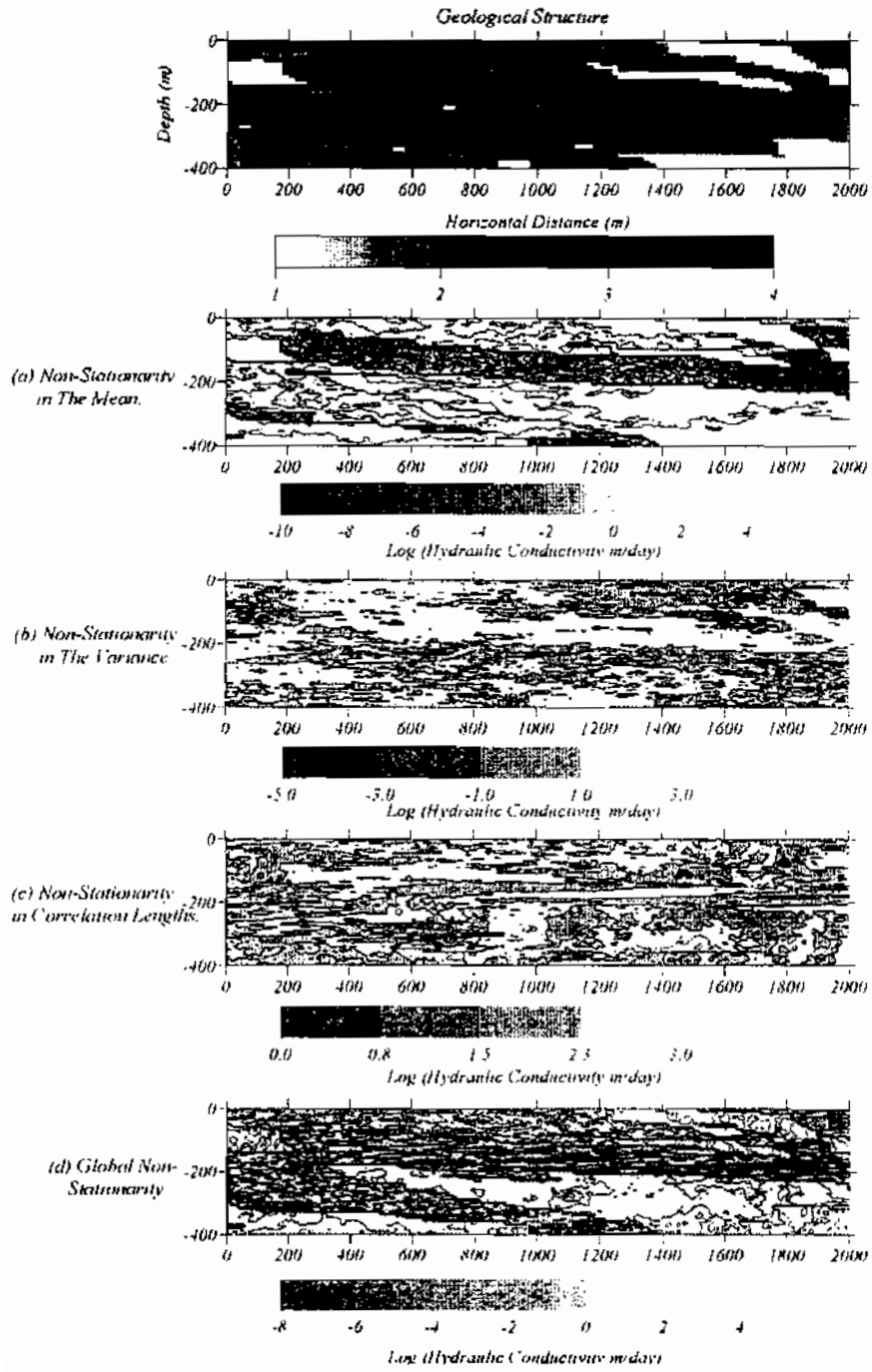
A. M. M. Elefkl

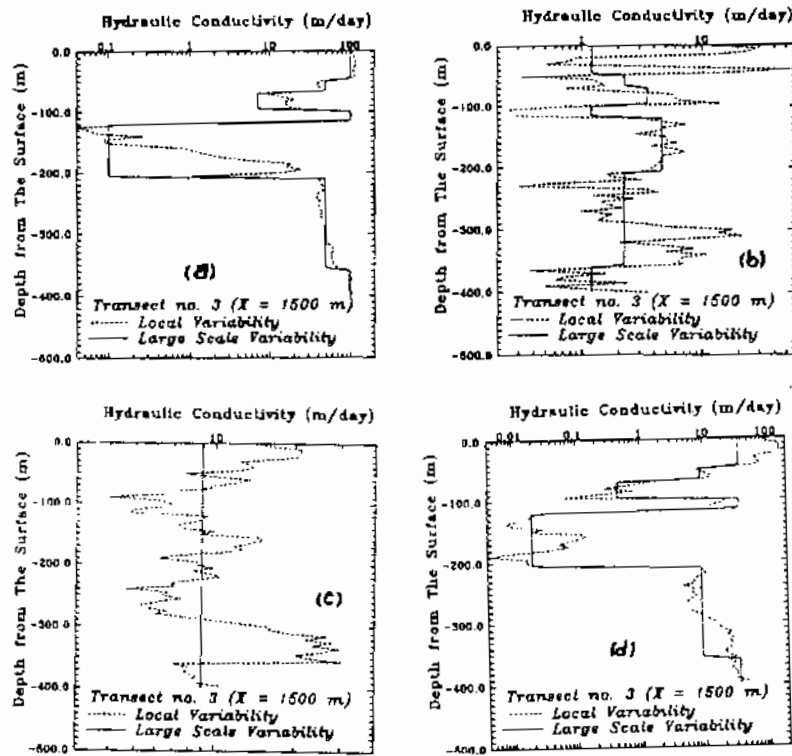Fig.1 Demonstration of The Hybrid Model with Some Synthetic Cases.

Fig.2 Conductivity Profiles for All Cases: (a) Nonstationarity in the Mean, (b) Nonstationarity in The Variance, (c) Nonstationarity in Correlation Lengths, (d) Global Nonstationarity.
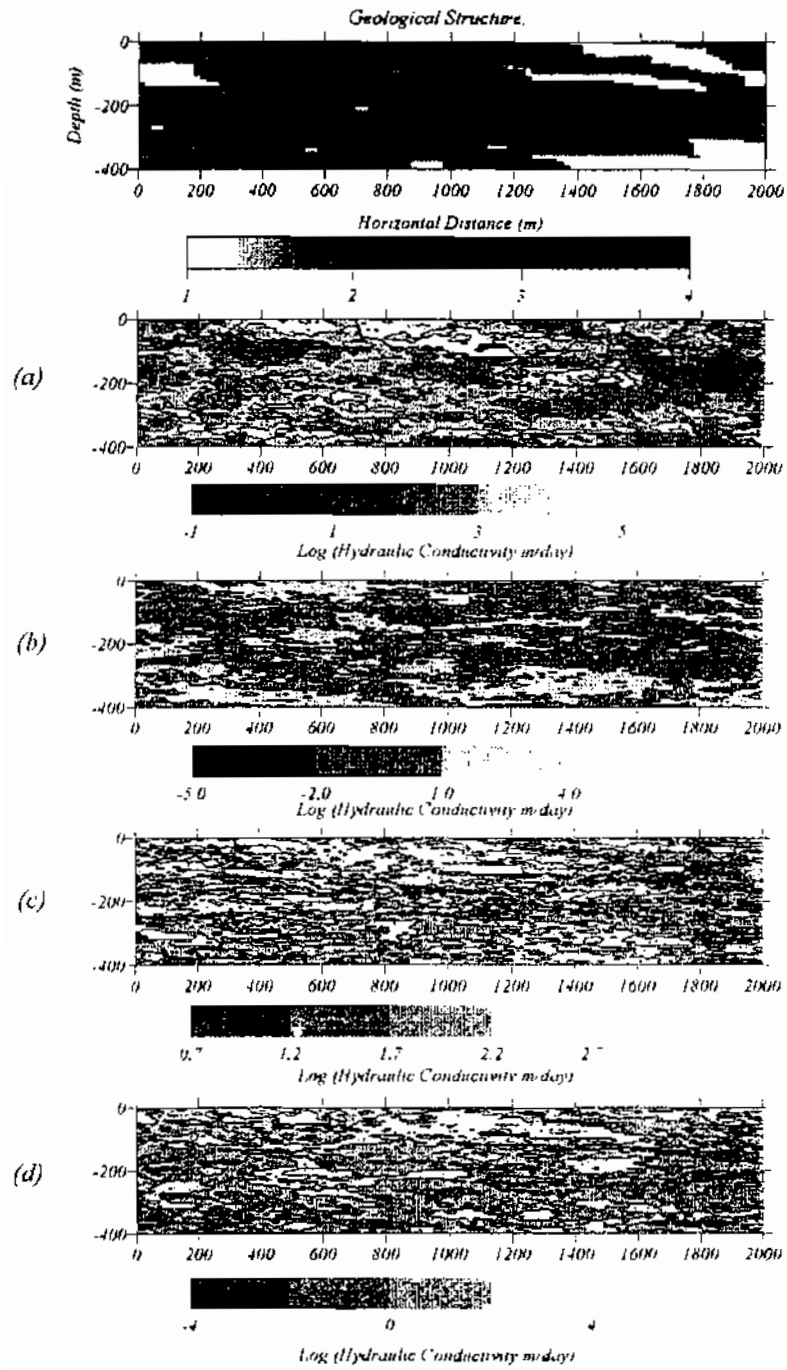
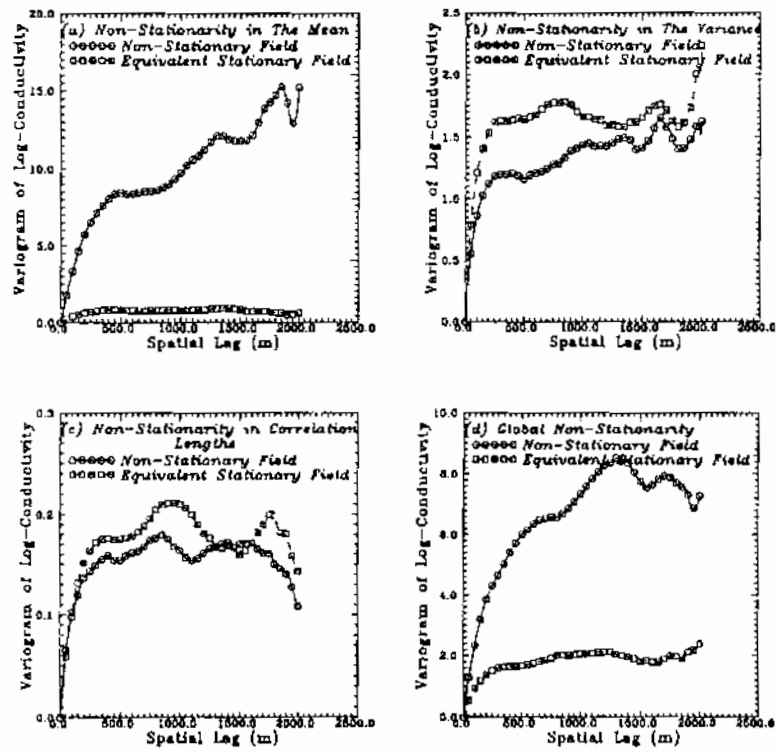Fig.3 Equivalent Stationary Fields of The Synthetic Examples.

Fig.4 Variograms of Log-Conductivity for All Cases in X-direction.